Energy Transfer from $N_2(v)$ to ClN_3 and a Kinetic Model for the Chain Decomposition of Chlorine Azide

R. H. Jensen, A. Mann, and R. D. Coombe*

Department of Chemistry and Biochemistry, University of Denver, Denver, Colorado 80208

Received: June 30, 1999; In Final Form: March 27, 2000

A number of experiments have been performed in an effort to better understand the photoinitiated chain decomposition of ClN_3. Discharge-flow methods were used to determine the rate of energy exchange between vibrationally excited N_2 (a likely chain carrier) and ClN_3. The rate constant for energy transfer from $N_2(v=1)$ to ClN_3 was found to be $(2.0 \pm 1.0) \times 10^{-13}$ cm^3 s^{-1} at 300 K. This process is thought to excite the ν_2 mode in ClN_3 with the release of 281 cm^{-1} of excess energy. Experiments were also performed in which the decomposition of ClN_3 was initiated by photolysis with a pulsed KrF laser at 249 nm, with subsequent observation of the time dependence of the densities of ClN_3, electronically excited NCl($a^1\Delta$), and vibrationally excited $ClN_3(\nu_2)$. A kinetic model for the ClN_3 decomposition was assembled based on reactions with NCl($a^1\Delta$) and $N_2(v)$.

Introduction

Although azides (RN_3) are well-known energetic species prone to explosive decomposition, the energy stored by these molecules has been used for many applications other than explosives. In particular, azides have recently been used as energetic precursors for the low-temperature deposition of thin films[1,2] and as energy storage agents for the pumping of new laser systems.[3] In our laboratory, chlorine azide (ClN_3) has been used as a source of electronically excited NCl($a^1\Delta$), a metastable species which can collisionally excite iodine atoms to the $5^2P_{1/2}$ state.[4] Under appropriate circumstances, a population inversion can be achieved among the $5^2P_{1/2}$ and $5^2P_{3/2}$ levels in this system and lasing is observed[3] at 1.315 μm. The operation of the laser requires that the ClN_3 initially present be removed since it is an efficient quencher of excited $I^*(5^2P_{1/2})$. This removal is thought to occur by chain decomposition processes.

It has been speculated[5,6] that the chain decomposition of azides is driven by energy transfer processes involving excited dissociation fragments, in particular vibrationally excited N_2. The vibrational frequency in N_2 (2331 cm^{-1}) is near-resonant with the ν_2 vibration in azides, which typically is found in the range from 2000 to 2150 cm^{-1}. This vibration is an asymmetric stretch along the N_3 chain and is well mapped onto the dissociation coordinate leading to the nitrene NR and N_2, such that sequential excitation by collisions with $N_2(v>0)$ might well lead to dissociation. Benard and co-workers[6] have speculated that this mechanism is responsible for the chain decomposition of FN_3 observed in high-temperature shock tube studies. Also, flowing streams of $N_2(v)$ have been used to dissociate gas phase NCN_3 for the deposition of C_3N_4 thin films.[2] In the case of ClN_3, the ν_2 frequency is 2050 cm^{-1} and excitation of this vibration by collisions with $N_2(v)$ is exothermic by 281 cm^{-1}. Since the binding energy of $ClN_3(^1A')$ along the coordinate leading to NCl($a^1\Delta$) + $N_2(X^1\Sigma_g^+)$ has been calculated[7] to be just 5700 cm^{-1}, sequential excitation of ClN_3 by as few as three collisions with $N_2(v)$ might dissociate the molecule. Further, since considerable energy is released when this dissociation occurs, it seems quite likely that $N_2(v)$ would be regenerated to continue the chain.

Because of the weakness of the $ClN-N_2$ bond, ClN_3 can also be dissociated by collisions with species in low-energy excited electronic states. It has been shown,[5] for example, that ClN_3 is dissociated by collisions with $O_2(a^1\Delta_g)$ to produce N_2 and NCl($a^1\Delta$). This process occurs with a room temperature rate constant near 10^{-11} cm^3 s^{-1}. Similarly, it has been suggested[4,5] that ClN_3 can be dissociated by collisions with NCl($a^1\Delta$) or with $I^*(5^2P_{1/2})$. I* quenching by ClN_3 has a rate constant[4] $k = 2.0 \times 10^{-11}$ cm^3 s^{-1}, and it is thought that this process also dissociates the azide to N_2 and NCl($a^1\Delta$). In our previous work[3] on the ClN_3/NCl($a^1\Delta$)/I* laser system, a kinetic model was assembled which included ClN_3 chain decomposition carried by $N_2(v)$, NCl($a^1\Delta$), and I*. Although the model was largely speculative (rate constants for energy exchange between $N_2(v)$ and ClN_3 were unknown, as was the time dependence of ClN_3 in the system), it gave fair agreement with the NCl($a^1\Delta$) time profile observed in the experiments and predicted laser threshold times within a factor of 2 of the observed values.

We have continued to explore these issues by using discharge-flow methods to determine the rate constant for energy transfer from $N_2(v)$ to ClN_3, and by using pulsed laser photolysis methods to perform additional measurements of the decomposition of this azide. In the latter case, measurements of the time decay of ClN_3 in the system were performed and vibrational excitation in the ν_2 mode of the azide was detected. Time profiles for ClN_3, NCl($a^1\Delta$), and $ClN_3(\nu_2)$ were measured for a variety of initial conditions. The data from both the discharge-flow and laser photolysis experiments were used to assemble a new kinetic model for the decomposition.

Experimental Details

Gaseous ClN_3 was synthesized by the passage of a stream of Cl_2 diluted in He (5% Cl_2) and saturated with H_2O over NaN_3 suspended on glass wool. The azide generator was derived from a design developed by Schlie and co-workers and has been described elsewhere.[8] The efficiency with which Cl_2 was converted to ClN_3 in the reactor was greater than 90%, as determined by IR and UV spectra of the effluent. The principal impurity present is expected to be Cl_2; in fact, no Cl_2 was

10.1021/jp992253o CCC: $19.00
Published on Web 06/22/2000

detected in the UV spectra and the 90% conversion figure is a minimum determined from signal-to-noise considerations. Continuously flowing streams of ClN_3/He from this reactor were used in the several different experiments of this study.

Experiments involving measurements of the rates of energy transfer from $N_2(v)$ were performed with a 1.0 m long, 3.8 cm internal diameter Pyrex discharge-flow reactor. Flows of $N_2(v)$ were generated by passage of N_2/He mixtures (typically 10% N_2) through a water-cooled 300 mA dc discharge positioned on a sidearm of the flow reactor. After exiting the discharge zone, the flow of excited gases was passed over a Ni mesh to remove atoms and electronically excited species.[9] $N_2(v)$ was detected downstream of the discharge by admitting a small flow of CO_2 to the flow via a sliding injector, such that the subsequent energy exchange produced vibrationally excited CO_2 which was detected at an observation port downstream by its emission on the ν_3 band near 4.3 μm. This emission was chopped at 343 Hz and detected with a cooled InSb detector equipped with a narrow band interference filter centered on the CO_2 transition. The response of the detector was amplified by a lock-in amplifier (Stanford Research Systems) and displayed on a strip chart recorder. Flows of ClN_3/He (5% ClN_3 as above) were admitted to the reactor via a second injector 10 cm downstream of the CO_2 injector.

The flows of all gases admitted to the reactor were measured with calibrated mass flow meters (Tylan and MKS). The system was pumped by a 1500 L min^{-1} mechanical pump such that the flow velocity for the pressures of the experiments (typically near 0.7 Torr) was approximately 1250 cm s^{-1}. The pressure in the system was measured with a capacitance manometer.

Laser photodissociation experiments were performed by photolysis of the ClN_3/He mixtures with the output of a pulsed KrF excimer laser at 249 nm (Questek). The photolysis cell was a 2.54 cm diameter Pyrex tube equipped with quartz windows for transmission of the 249 nm laser beam and KCl windows for transmission of the IR probe beam used for detection of the ClN_3 and for transmission of IR emissions from the gases in the cell. IR absorption was detected on the ν_2 band of ClN_3 near 2050 cm^{-1} by using a source constructed from a heated wire and a detector comprised of a cooled InSb detector with a narrow band interference filter centered at this frequency. Calibrations of the absorption measurement were done repeatedly over the course of the experiments by comparison of IR absorptions with densities of ClN_3 determined from measured UV absorptions and published UV absorption cross sections.[10] Emission from vibrationally excited ClN_3 was observed using the same detector and filter combination, but with the IR source blocked. Emission from electronically excited $NCl(a^1\Delta)$ at 1.077 μm was detected by a cooled Ge detector (North Coast Optics) equipped with a narrow band filter centered at this wavelength and with a bandwidth (full width half-maximum) of 12 nm. The time profiles of emission and absorption signals were amplified and digitized with a LeCroy TR8828C signal processor.

Results

1. Quenching of $N_2(v)$ by ClN_3. Vibrationally excited N_2 was generated using the dc discharge flow reactor described above, with detection by the admission of CO_2 to the flow. The total density of N_2 in the flow was typically set at 2.3×10^{15} cm^{-3}. The density of the added CO_2 was near 1.0×10^{14} cm^{-3}. For the conditions of our experiments, the intensity of 4.3 μm emission from vibrationally excited $CO_2(\nu_3)$ should be proportional to the density of vibrationally excited $N_2(v)$ in the system. The energy exchange between $N_2(v=1)$ and CO_2 is nearly resonant (exothermic by 18 cm^{-1} for the forward process) and for sufficient densities of both species full equilibration would result. From the known values[11] of the rate constants for the forward and reverse reactions and the densities of N_2 and CO_2 in the system, the equilibrium should be established within 1.0 ms, comparable to the mixing time. The decay of the emission reflects the loss of energy from this equilibrium pool, largely by radiation from the excited CO_2. A steady-state treatment of the $CO_2(v)$ density yields the following expression:

$$[CO_2(v)]_{ss} = k_e[N_2(v)][CO_2]/\{k_{-e}[N_2] + k_r\} \qquad (1)$$

where k_e and k_{-e} are rate constants for the forward and reverse energy transfer reactions, respectively, and the rate of spontaneous emission (k_r) for an isolated $CO_2(\nu_3,v=1)$ molecule is 417 s^{-1} ($\tau = 2.4$ ms).[12] Hence $[CO_2(v)]$ (and the intensity of its IR emission) should vary in proportion to $[N_2(v)]$. By using values of k_e and k_{-e} from the literature[11] and the densities of N_2 and CO_2 from the experiments, eq 1 yields the steady-state ratio $[CO_2(v)]/[N_2(v)] = 0.039$. Because of the relatively high density of N_2 in the system, the large majority of the excitation resides in $N_2(v)$. Since only 0.039 of the vibrational excitation resides in CO_2 at any time, the decay of the equilibrium pool of vibrationally excited species (observed by the $CO_2(v)$ emission intensity) will reflect the $CO_2(v)$ radiative rate (k_r) multiplied by this factor. This treatment yields a decay rate of 17 s^{-1}. The decay rate observed in the present experiments was 20 s^{-1}, in good agreement with this predicted result. The small discrepancy may in fact indicate the contribution of some other loss mechanism such as wall quenching of $CO_2(v)$, for which the reported probability is 0.22 per collision for a variety of surfaces.[13]

Quenching experiments were performed by addition of ClN_3 to the $N_2(v)$ stream at a point 10 cm (8 ms) downstream of the CO_2 injector. The ClN_3 inlet was positioned 22.5 cm (18 ms) upstream of the observation port. The presence of ClN_3 at densities up to 2.5×10^{14} cm^{-3} (the maximum from our azide generator) resulted in substantial reductions in the intensity of the CO_2 emission, indicating quenching of the $N_2(v)$ since the large majority of the excitation is resident in this species. Considering only the vibrational energy exchange between ClN_3 and $N_2(v)$, the rate equation for $N_2(v)$ is given by

$$d[N_2(v)]/dt = -k_9[N_2(v)][ClN_3] + k_{-9}[N_2][ClN_3(v)] \qquad (2)$$

where k_9 and k_{-9} are rate constants for the forward and reverse energy transfer processes. In this case the forward process is exothermic by 281 cm^{-1}. A steady-state treatment of the $ClN_3(v)$ density yields an expression analogous to eq 1 above:

$$[ClN_3(v)]_{ss} = k_9[N_2(v)][ClN_3]/(k_{-9}[N_2] + k_q) \qquad (3)$$

where k_q represents the rate of first-order losses of $ClN_3(v)$ by radiation and collisional quenching. Substitution of eq 3 in eq 2 yields

$$d[N_2(v)]/dt = \alpha[N_2(v)][ClN_3] \qquad (4)$$

where

$$\alpha = -k_9\{1 - k_9k_{-9}[N_2]/(k_{-9}[N_2] + k_q)\} \qquad (5)$$

Hence the density of $N_2(v)$ should decay as $\exp(\alpha[ClN_3]t)$, and a plot of $\ln[N_2(v)]$ (i.e., ln(intensity)) vs $[ClN_3]$ for a fixed time t should be linear with slope αt.

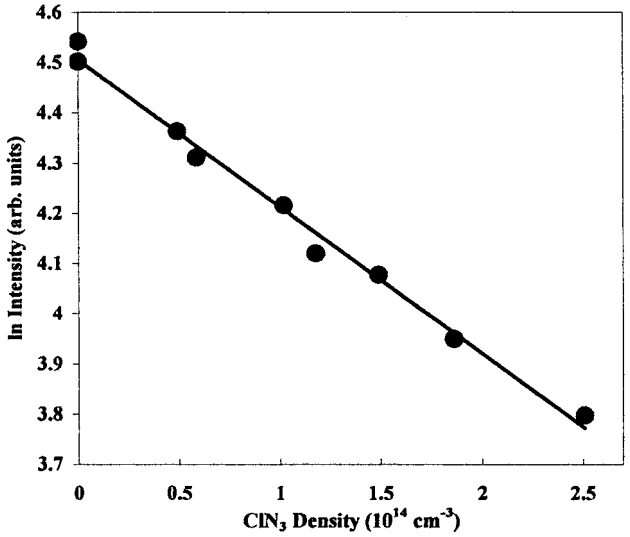

Figure 1. A plot of the natural log of the intensity of emission from $CO_2(\nu_3)$ vs the density of ClN_3, measured at $t = 0.018$ s after admission of ClN_3 to the flow.

Figure 1 shows the results of experiments in which the emission intensity was measured at $t = 0.018$ s for various densities of ClN_3. The plot is in fact linear and the slope (αt) yields a value $\alpha = -1.63 \times 10^{-13}$ cm^3 s^{-1}. The value of the energy transfer rate constant k_9 can be determined from α if the first-order $ClN_3(v)$ quenching rate k_q is known. Careful comparison of the frequency-integrated infrared absorption strengths of the ν_2 and ν_3 bands of ClN_3 and CO_2 indicates that the transition in ClN_3 is 4.8 times stronger than that in CO_2, suggesting that the radiative rate of excited $ClN_3(\nu_2,v=1)$ is greater than that of $CO_2(\nu_3,v=1)$ by this same factor, i.e., $k_q \approx 2000$ s^{-1}. Using this result and the relationship between k_9 and k_{-9} ($k_{-9} = k_9 \exp(-281\ \text{cm}^{-1}/kT)$), a value $k_9 = 1.7 \times 10^{-13}$ cm^3 s^{-1} is obtained. This result is in fact reasonably insensitive to the value of k_q; for $k_q = 500$ s^{-1}, $k_9 = 2.0 \times 10^{-13}$ cm^3 s^{-1}. Considering all of the uncertainties in the experiments and the treatment of the results, $k_9 = (2.0 \pm 1.0) \times 10^{-13}$ cm^3 s^{-1}.

2. Laser Photodissociation Experiments. Photodissociation of ClN_3 using excimer laser sources at 193 or 249 nm has been performed a number of times in the past,[5,10] and it is known that the principal photofragments are $NCl(a^1\Delta)$ and $N_2(X^1\Sigma^+_g)$. Coombe and co-workers[10] reported some dissociation to triplet fragments $NCl(X^3\Sigma^-) + N_2(A^3\Sigma^+_u)$, but this channel is believed to be minor[14] and the density of $N_2(A)$ metastables very small relative to $NCl(a^1\Delta)$. More recently, Ray and Coombe[5] investigated the chain decomposition of ClN_3 after photolysis at 193 and 249 nm, and found the latter wavelength to be more efficient at initiation of the chain. In the present experiments, 249 nm photolysis was used once again for the photodissociation of samples of ClN_3/He (5% ClN_3) at densities of the azide up to 1.61×10^{16} cm^3 and incident laser fluences up to a maximum of 13.5 mJ/cm^2. These conditions correspond to photodissociation of a maximum of 2.7% of the ClN_3 initially present.[10] Time profiles were recorded of the density of the ClN_3 parent using the IR absorption method described above, in addition to time profiles of IR emissions from $NCl(a^1\Delta)$ and vibrationally excited $ClN_3(\nu_2)$ for many different combinations of initial ClN_3 densities and incident laser fluences. Typical data are presented in Figures 2, 4, and 6.

Figure 2 shows time profiles of the change in the ClN_3 density recorded by IR absorption, for initial densities ranging from 6.44×10^{15} to 1.61×10^{16}cm^{-3} at a fixed fluence of 13.5 mJ/cm^2. The ClN_3 density declines over a period of 500 μs after

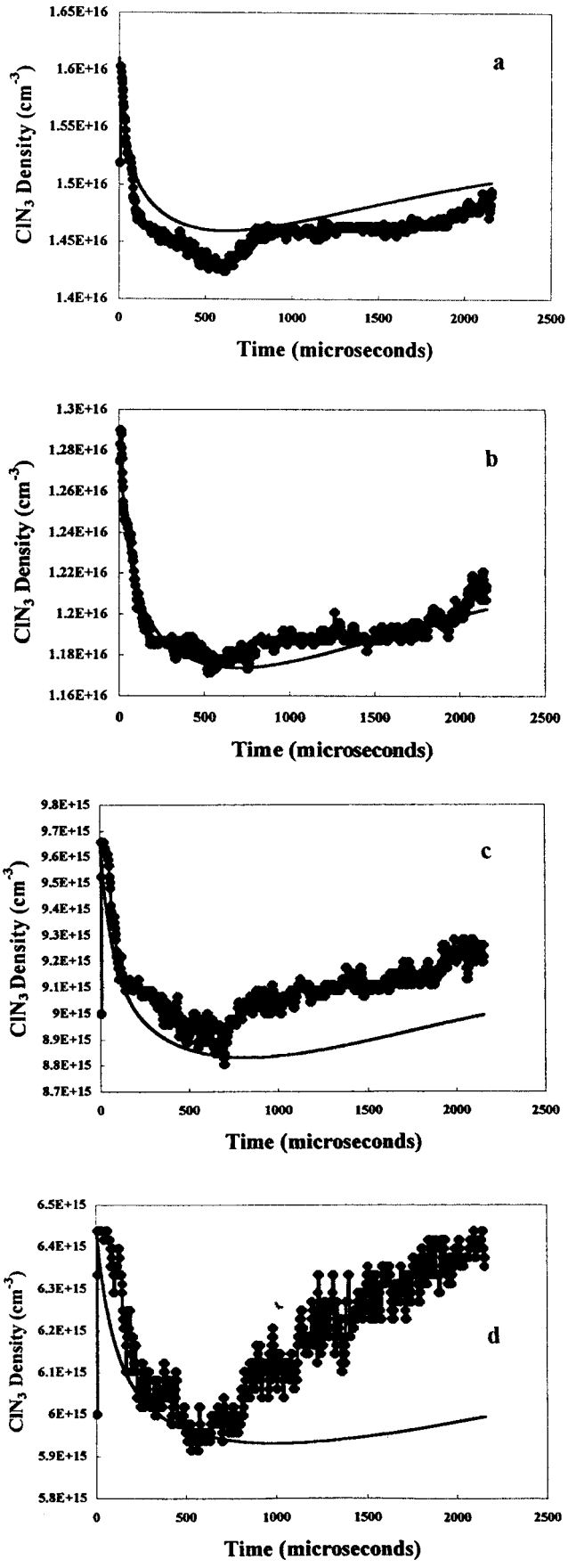

Figure 2. Time profiles of the densities of $ClN_3(v=0)$ for four initial ClN_3 densities photolyzed at 249 nm: (a) $[ClN_3]_0 = 1.61 \times 10^{16}$, (b) $[ClN_3]_0 = 1.29 \times 10^{16}$, (c) $[ClN_3]_0 = 9.66 \times 10^{15}$, (d) $[ClN_3]_0 = 6.44 \times 10^{15}$ cm^{-3}. Corresponding time profiles computed from the kinetic model are shown as solid lines.

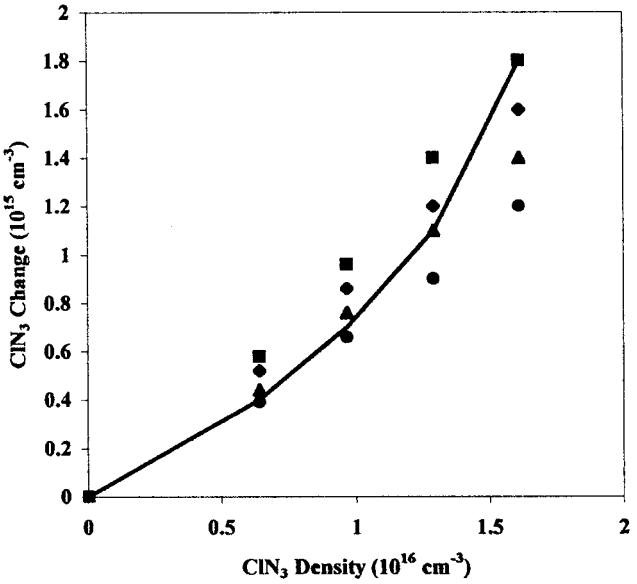

Figure 3. Plots of the change in the density of ClN_3 at 500 μs after the laser pulse (i.e., $[ClN_3]_0 - [ClN_3]_{500\ \mu s}$) vs the initial density of ClN_3, for photolysis at 249 nm and 2.7% initial dissociation. Experimental data are shown by the solid line. (■), (♦), (▲), (●) correspond to values computed from the kinetic model for $k_7 = 3.0 \times 10^{-12}$, 2.5×10^{-12}, 2.0×10^{-12}, and 1.5×10^{-12} cm^3 s^{-1}, respectively.

the photolysis pulse and the overall loss of the azide reaches more than four times that from the initial photodissociation (2.7%), suggesting the operation of a chain. The removal of the ClN_3 from the system is incomplete, with the IR absorbance reaching a minimum and then increasing again beyond 1 ms in each case. The proportion of the ClN_3 removed by the chain was observed to increase with the initial density of the azide (hence the initial density of photofragments). Figure 3 shows a plot of the change in the density of ClN_3 at a fixed time after the laser pulse (500 μs) vs the initial density of ClN_3, for a fluence of 13.5 mJ/cm^2. For the data shown, the proportion of ClN_3 removed varies from 6.2% for the lowest initial density to 11.2% for the highest initial density.

Figure 4 shows a typical time profile of the density of NCl($a^1\Delta$) observed via its emission at 1.08 μm. Such data were obtained for a range of initial ClN_3 densities and laser fluences. The data shown are for an initial ClN_3 density of 6.44×10^{15} cm^{-3} and a fluence of 13.5 mJ/cm^2. The time profile exhibits a very rapid decline over 200 μs followed by a much more slowly decaying, lower intensity "tail" extending beyond 2 ms. The rise time of the initial intense peak corresponds to the time constant of the Ge detector used in the experiments, 13 μs. All of the NCl($a^1\Delta$) time profiles observed in the experiments were well fitted by a sum of two exponential decays (intensity $= A_1 \exp(-\lambda_1 t) + A_2 \exp(-\lambda_2 t)$). Figure 4 also shows a plot of ln(intensity) vs time, with lines indicating the two distinct linear components. Plots of the exponential decay rate of the initial intense component vs laser fluence for four different initial ClN_3 densities are shown in Figure 5. Note that for the higher density data, the decays become *slower* with increasing fluence. For the conditions of the experiments, increasing fluence corresponds to increasing initial densities of the photofragments NCl($a^1\Delta$) and $N_2(v)$ with a nearly constant density of ClN_3. This result suggests that the initial NCl($a^1\Delta$) decay is not dominated by second-order processes among the photofragments (for which the rate would increase with increasing fluence), but rather by pseudo-first-order interactions with ClN_3, and that interactions between the photofragments and ClN_3 mitigate this decay by

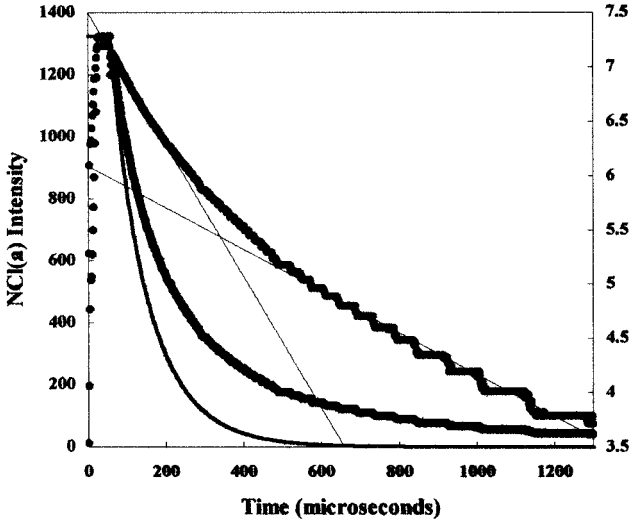

Figure 4. Time profile of emission from NCl($a^1\Delta$) from 249 nm photolysis of ClN_3, for an initial ClN_3 density of 6.44×10^{15} cm^{-3}. Also shown is a plot of the natural log of the emission intensity vs time, with thin lines indicating the slopes at short and long times after the laser pulse (units of the logarithmic scale are shown on the right axis). The time profile computed from the model is shown as a thick solid line.

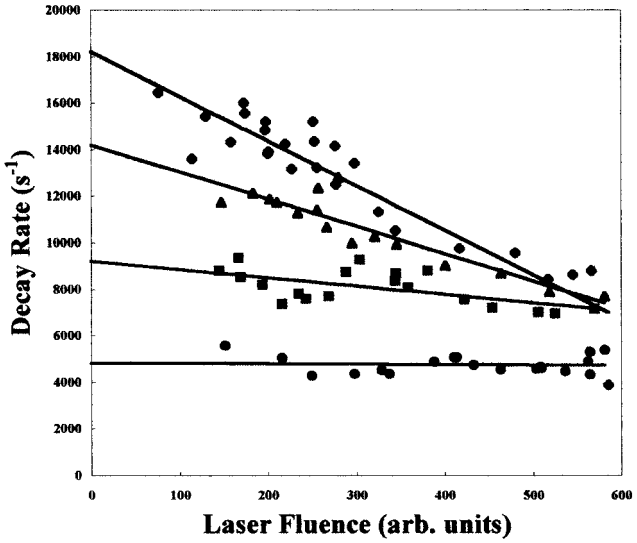

Figure 5. Plots of the experimental decay rate of the fast component of the NCl($a^1\Delta$) time decay vs the fluence of the photolysis laser, for four different initial densities of ClN_3: (♦) $[ClN_3]_0 = 1.29 \times 10^{16}$ cm^{-3}; (▲) $[ClN_3]_0 = 9.66 \times 10^{15}$ cm^{-3}; (■) $[ClN_3]_0 = 6.44 \times 10^{15}$ cm^{-3}; (●), $[ClN_3]_0 = 3.22 \times 10^{15}$ cm^{-3}. The lines shown are least-squares fits to the data.

some regeneration of NCl($a^1\Delta$) at higher fluences. For the lower initial ClN_3 densities, the NCl($a^1\Delta$) decay exhibits virtually no dependence on laser fluence, suggesting that under these circumstances processes which regenerate NCl($a^1\Delta$) simply do not compete with pseudo-first-order quenching.

Figure 6 shows the time profile of emission from vibrationally excited $ClN_3(\nu_2)$, observed via its IR emission near 4.7 μm, for a ClN_3 density of 1.61×10^{16}cm^{-3} and a fluence of 13.5 mJ/cm^2. Also shown is absorption data indicating loss of ground state ClN_3 for these same conditions. The two time profiles are clearly related, the initial growth in $ClN_3(\nu_2)$ tracking the decay in ClN_3. The $ClN_3(\nu_2)$ emission was observed to extend well beyond 2 ms after the photolysis pulse. It exhibits oscillatory behavior after an initial rise over about 200 μs, and indeed the oscillations appear to be evident in the ground-state ClN_3

TABLE 1: Kinetic Model for the ClN_3 Chain

initiation	
$ClN_3 + h\nu \rightarrow NCl(a^1\Delta) + N_2(v)$	
propagation	
$NCl(a^1\Delta) + ClN_3 \rightarrow NCl(X^3\Sigma^-) + NCl(a^1\Delta) + N_2(v)$	$k_7 = 2.0 \times 10^{-12}$ cm^3 s^{-1}
$\rightarrow NCl(X^3\Sigma^-) + ClN_3(v=1)$	$k_8 = 1.5 \times 10^{-12}$ cm^3 s^{-1}
$N_2(v) + ClN_3 \rightarrow ClN_3(v=1) + N_2$	$k_9 = 2.0 \times 10^{-13}$ cm^3 s^{-1}
$N_2(v) + ClN_3(v=1) \rightarrow ClN_3(v=2) + N_2$	$k_{10} = 2.0 \times 10^{-13}$ cm^3 s^{-1}
$N_2(v) + ClN_3(v=2) \rightarrow NCl(a^1\Delta) + N_2(v) + N_2$	$k_{11} = 2.0 \times 10^{-13}$ cm^3 s^{-1}
termination	
$NCl(a^1\Delta) + NCl(a^1\Delta) \rightarrow N_2(v) + 2Cl$	$k_{12} = 8.0 \times 10^{-12}$ cm^3 s^{-1}
$NCl(a^1\Delta) \rightarrow NCl(X^3\Sigma^-)$	$k_{13} = 500$ s^{-1}
$ClN_3(v=1) \rightarrow ClN_3(v=0)$	$k_{14} = 500$ s^{-1}
$ClN_3(v=2) \rightarrow ClN_3(v=1)$	$k_{15} = 2000$ s^{-1}

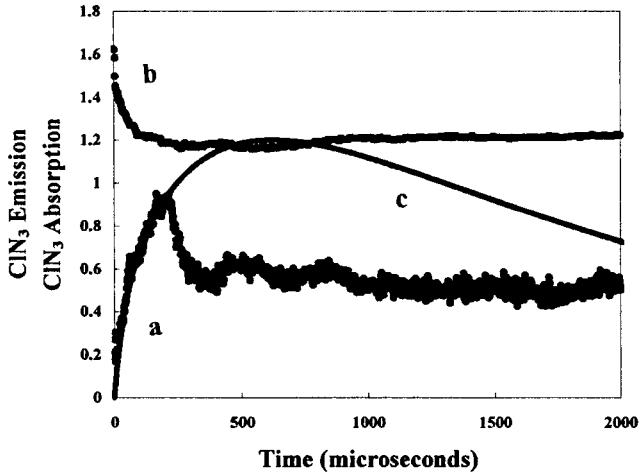

Figure 6. (a) Time profile of IR emission from vibrationally excited $ClN_3(\nu_2)$ for 249 nm photolysis of $[ClN_3]_0 = 1.61 \times 10^{16}$ cm^{-3}. (b) The corresponding time profile of the density of $ClN_3(v = 0)$ from IR absorbance. (c) Time profile of $ClN_3(\nu_2,v=1)$ computed from the kinetic model. Units on the vertical axis are arbitrary.

absorption as well (Figure 2). This remarkable phenomenon was reproducible under a variety of density and fluence conditions.

3. Kinetic Model. Our objective was to assemble the simplest possible kinetic model consistent with the major features of the data, based on known rate constants and reasonable assumptions about processes for which rate constants are unknown. A summary of the model is presented in Table 1. We assume that initiation of the chain begins with photolysis of ClN_3 to produce both $NCl(a^1\Delta)$ and vibrationally excited N_2:

$$ClN_3 + h\nu(249\text{ nm}) \rightarrow NCl(a^1\Delta) + N_2(v) \qquad (6)$$

The generation of $N_2(v)$ in this process seems reasonable in light of the large amount of energy released beyond that required for the production of $NCl(a^1\Delta)$ and the difference in bond lengths between N_2 and the terminal N−N bond in the azide.[15]

The chain can be propagated by either of the two photofragments. By analogy with the reactions[5] of ClN_3 with $O_2(a^1\Delta_g)$ and $I^*(5^2P_{1/2})$, reaction of the azide with $NCl(a^1\Delta)$ is expected to be much faster than vibrational energy exchange between ClN_3 and $N_2(v)$. Indeed, the initial decline of the ClN_3 absorbance (Figure 2) tracks the initial decay of the $NCl(a^1\Delta)$ emission signal (Figures 4 and 5), supporting the idea that the $NCl(a^1\Delta)/ClN_3$ interaction dominates the chemistry of the system immediately after the photolysis pulse. We note also that the initial rise of the $ClN_3(v=1)$ emission signal (Figure 6) tracks the initial decays of $NCl(a^1\Delta)$ and $ClN_3(v=0)$, suggesting that its production involves an electronic-to-vibrational energy transfer process among these two species. Hence, we postulate that the following reactions occur:

$$NCl(a^1\Delta) + ClN_3 \rightarrow NCl(X^3\Sigma^-) + NCl(a^1\Delta) + N_2(v) \qquad k_7 = 2.0 \times 10^{-12}\text{ cm}^3\text{ s}^{-1} \quad (7)$$

$$\rightarrow NCl(X^3\Sigma^-) + ClN_3(v=1) \qquad k_8 = 1.5 \times 10^{-12}\text{ cm}^3\text{ s}^{-1} \quad (8)$$

Process 7 is analogous to the reaction between ClN_3 and $O_2(a^1\Delta_g)$, and process 8 is $E-V$ energy exchange. The values of k_7 and k_8 were determined from the present data as described below.

Chain propagation by $N_2(v)$ would involve vibrational excitation of the ClN_3 in sequential collisions with this species, with the third such collision resulting in dissociation:

$$N_2(v) + ClN_3 \rightarrow N_2 + ClN_3(v=1) \qquad k_9 = 2 \times 10^{-13}\text{ cm}^3\text{ s}^{-1} \quad (9)$$

$$N_2(v) + ClN_3(v=1) \rightarrow N_2 + ClN_3(v=2) \qquad k_{10} = 2 \times 10^{-13}\text{ cm}^3\text{ s}^{-1} \quad (10)$$

$$N_2(v) + ClN_3(v=2) \rightarrow N_2 + NCl(a^1\Delta) + N_2(v) \qquad k_{11} = 2 \times 10^{-13}\text{ cm}^3\text{ s}^{-1} \quad (11)$$

Here we assume the barrier height reported by Benard and coworkers.[7] The rate constants assigned to processes 9, 10, and 11 are given by the value obtained from the present data as described above. Since the density of ground-state N_2 in the system is very much smaller than that of ClN_3, we have neglected the endothermic reverse of reaction 9.

Chain termination steps include those processes that remove $NCl(a^1\Delta)$, $N_2(v)$, $ClN_3(v=1)$ or $ClN_3(v=2)$ from the system. The best known such process is the $NCl(a^1\Delta)$ "self-annihilation" reaction:

$$NCl(a^1\Delta) + NCl(a^1\Delta) \rightarrow N_2(v) + 2Cl \qquad k_{12} = 8.0 \times 10^{-12}\text{ cm}^3\text{ s}^{-1} \quad (12)$$

where the rate constant is that reported by Benard and co-workers.[7] We have also included in the model first-order processes that remove the chain carriers, as follows:

$$NCl(a^1\Delta) \rightarrow NCl(X^3\Sigma^-) \qquad k_{13} = 500\text{ s}^{-1} \qquad (13)$$

$$ClN_3(v=1) \rightarrow ClN_3(v=0) \qquad k_{14} = 500\text{ s}^{-1} \qquad (14)$$

$$ClN_3(v=2) \rightarrow ClN_3(v=1) \qquad k_{15} = 2000\text{ s}^{-1} \qquad (15)$$

These processes are intended to reflect losses by radiation, wall

quenching, and pseudo-first-order quenching by collisions with species present in the reaction mixture. The values of k_{14} and k_{15} reflect IR radiation from excited ClN_3. At the densities of the pulsed experiments, considerable radiation trapping is expected for the $v = 1 \rightarrow v = 0$ transition in this molecule. This phenomenon is well-known for CO_2, and k_{14} was determined by multiplying the reported[16] radiation-trapped rate for CO_2 by the factor of 4.8 noted above. The flow reactor experiments described above indicate that $N_2(v)$ quenching is very slow, even on Pyrex walls. Hence, mechanisms for loss of $N_2(v)$ have not been included in the model. The value of k_{13} is an estimate reflecting slow loss of $NCl(a^1\Delta)$ by collisions with walls or impurities present.

The rate constants indicated above for reactions 7 and 8 are key to the model and were determined from the present data. Because reaction of $NCl(a^1\Delta)$ with ClN_3 is much faster than vibrational energy transfer between $N_2(v)$ and ClN_3, the chain mechanisms carried by these two species are separated in time from one another. The initial loss of ClN_3 in the system evident in Figure 2 is dominated by the relatively fast processes involving $NCl(a^1\Delta)$. Since reaction 7 does not result in loss of $NCl(a^1\Delta)$ from the system, the initial losses of both $NCl(a^1\Delta)$ and ClN_3 must correspond to reaction 8. The rate constant k_8 can thus be inferred from the observed exponential decay rates of the rapid decay component of the $NCl(a^1\Delta)$ emission for different initial ClN_3 densities in the limit of zero laser fluence (i.e., in the limit where no secondary reactions occur), Figure 5. The zero fluence intercepts of the four data sets shown all indicate rate constants between 1.42×10^{-12} and 1.49×10^{-12} $cm^3\ s^{-1}$. In the model, we have set $k_8 = 1.5 \times 10^{-12}$ $cm^3\ s^{-1}$.

The total loss of ClN_3 from the system in the first few hundred microseconds after the laser pulse is determined by both processes 7 and 8. With the value of k_8 set, The magnitude of k_7 can be determined by fitting the kinetic model to the data shown in Figure 2 (the overall loss of ClN_3). The coupled differential rate equations corresponding to reactions 7−15 were numerically integrated using a Runge−Kutta routine with adaptive step size control. The densities of ClN_3, $NCl(a^1\Delta)$, $N_2(v)$, $ClN_3(v=1)$, $ClN_3(v=2)$, Cl, and $NCl(X^3\Sigma^-)$ were computed at a minimum of 500 intervals over a total time of 3 ms. Initial conditions (the densities of ClN_3, $NCl(a^1\Delta)$, and $N_2(v)$) were chosen according to actual ClN_3 densities and incident laser fluences employed in the experiments. Since the laser output irradiated the full volume of the reaction vessel in the experiments, the initial densities were assumed to be spatially uniform. Figure 3 (the plot of the density of ClN_3 lost during the first 500 μs vs the initial azide density) also indicates the modeled results. The best fit to the experimental data is obtained for $k_7 = 2.0 \times 10^{-12}$ $cm^3\ s^{-1}$. Modeled results are also shown for $k_7 = 1.5 \times 10^{-12}$, 2.5×10^{-12}, and 3.0×10^{-12} $cm^3\ s^{-1}$ to indicate the sensitivity of this result.

The results of calculations with the complete model are shown with the corresponding experimental data in Figures 2, 4, and 6. The agreement between the data and the results of the model is reasonable. The magnitude of the overall reduction of the ClN_3 density (Figure 2) is reproduced well by the model, as is the time dependence of the ClN_3 density at short times after the laser pulse ($t < 750$ μs). Significant disagreement is evident at longer times, though, particularly for the lowest ClN_3 densities. It is apparent that the chain carried by $NCl(a^1\Delta)$ removes an amount of ClN_3 several times that removed by the initial photodissociation, and it would seem that the increase in the ClN_3 absorbance observed at longer times (>1.0 ms) corresponds to repopulation of $ClN_3(v=0)$ by radiation from higher vibrational levels. The model reproduces the fast initial decay of the $NCl(a^1\Delta)$ density (Figure 4), but it clearly does not reproduce the intensity of the slow component of the decay. The model predicts a significant $ClN_3(v=1)$ density (Figure 6) with a time profile that agrees very well with the initial rise of the emission signal observed in the experiments. The experimental signal exhibits the onset of oscillations with an abrupt decay beginning at about 200 μs, though, and this behavior is not reproduced by the model.

Discussion

The data described above show that the rate constant for quenching of $N_2(v)$ by ClN_3 has a magnitude $k_9 = (2 \pm 1) \times 10^{-13}$ $cm^3\ s^{-1}$ at 300 K. This value, together with the observation of emission from vibrationally excited $ClN_3(\nu_2)$, strongly suggests that the quenching process involves near-resonant vibration-to-vibration energy transfer. Sharma and Brau[17] have described such energy transfer processes in terms of the coupling of transitions in the colliding species by long-range intermolecular forces. For nearly resonant energy exchange ($\Delta\epsilon < 20$ cm^{-1}), the energy transfer rate constants are predicted to vary with the magnitudes of the transition dipole moments in the colliding molecules. For greater energy gaps, experiments have shown the rate constants to vary as $\exp(-\Delta\epsilon/kT)$. Since the energy gap for reaction 9 is 281 cm^{-1}, and that for $CO_2(v)$ energy transfer to N_2 is just 18 cm^{-1}, the rate constants for the two processes might be expected to be related by a factor $\exp(-281\ cm^{-1}/kT) = 0.26$ at room temperature. In fact, $k_9/k_{-e} = 0.34$, in reasonable agreement with this result. The difference suggests some contribution to k_9 from the greater transition moment in ClN_3 relative to CO_2.

From the data and the kinetic model, the overall rate constant for the reaction of $NCl(a^1\Delta)$ with ClN_3 is found to be 3.5×10^{-12} $cm^3\ s^{-1}$, with the channel that actually results in loss of $NCl(a^1\Delta)$ (reaction 8) having a branching fraction of (43 ± 10)%. Schlie and co-workers[8] have reported a rate constant $k = 5.7 \times 10^{-13}$ $cm^3\ s^{-1}$ for the removal of $NCl(a^1\Delta)$ in collisions with ClN_3, based on the results of experiments in which the $NCl(a^1\Delta)$ decay was measured after 193 nm photolysis of ClN_3. Similar results have been reported by Heaven et al.,[18] and by Coombe and van Benthem.[19] From Figure 5, though, it is apparent that the observed decays can vary substantially with laser fluence, with the decays becoming longer at higher fluences. Indeed, from the data in Figure 5, the apparent value of k_8 for $[ClN_3] = 1.6 \times 10^{16}$ and the highest laser fluence used in the present experiments is 5.6×10^{-13} $cm^3\ s^{-1}$, very near that reported by Schlie and co-workers.[8] For greater fluences, the apparent rate constant may be still smaller; Coombe and Van Benthem[19] report a rate constant of 1.25×10^{-13} $cm^3\ s^{-1}$ from experiments in which 14% of the ClN_3 initially present was photodissociated at 193 nm. Extrapolation to zero fluence is needed to remove the effect of regeneration of $NCl(a^1\Delta)$ by the chain.

In the model, we have indicated that quenching of $NCl(a^1\Delta)$ by collisions with ClN_3 proceeds by an $E-V$ energy exchange in which the azide is vibrationally excited. We note also, though, that flow reactor studies performed by Clyne and MacRobert[20] have shown that NCl reacts with Cl_2 to produce NCl_2, with a similar rate constant. An analogous reaction between NCl and ClN_3 would produce NCl_2 and N_3. We have indicated the products of the $NCl(a^1\Delta)$ self-annihilation (reaction 12) to be molecular nitrogen and Cl atoms. While the rate constant for this process is known,[7] its products are not. If Cl atoms are in fact produced, they can react with ClN_3 to generate Cl_2 and N_3.

This reaction has been studied with discharge-flow mass spectrometry methods,[21] and its rate constant is reported to be 3.5×10^{-12} cm^3 s^{-1} at 300 K. N_3 radicals generated by this process (or by NCl($a^1\Delta$) + ClN_3) can react[22] with Cl atoms to produce additional NCl($a^1\Delta$), enhancing the rate of the chain carried by the nitrene. Also, the N_3 radicals would themselves be removed by a self-annihilation process which would likely generate $N_2(v)$; the rate constant of this process is known[23] to be 2.0×10^{-12} cm^3 s^{-1}. These second-order processes are expected to have a minimal effect on the rate of loss of ClN_3 for low initial densities of chain carriers, as in the present experiments. Although they may well be important at higher fluences, we have chosen not to include them in the current mechanism since the density of Cl atoms actually present in the system is unknown, and may be small.

Heaven and co-workers[18] have recently reported experiments in which both NCl($a^1\Delta$) and NCl($X^3\Sigma^-$) were observed after 249 nm photolysis of ClN_3. These authors indicate that the NCl($a^1\Delta$) emission signals observed in their experiments suffer from interference from nearby features of the N_2 first positive ($B^3\Pi_g \rightarrow A^3\Sigma_u^+$) system, particularly the 0,0 band of this transition at 1.04 μm, in the first few hundred microseconds after the laser pulse. The filter used in observations of NCl($a^1\Delta$) in the present experiments (12 nm fwhm) should effectively block this N_2 emission. We note also that excited N_2 metastables are present in the system[10] at densities likely to be several orders of magnitude less than that of NCl($a^1\Delta$) and should not play a significant role in the loss of ClN_3 evident in Figure 2 above. The agreement between the ClN_3 and NCl($a^1\Delta$) time profiles observed in the present experiments lends support to the notion that the latter are not significantly contaminated by emission from excited N_2.

Both the data and the kinetic model indicate that the chain has a very limited impact on the system for low densities of chain carriers, as in the present experiments. Nonetheless, features like the long, slowly decaying tail of the NCl($a^1\Delta$) emission in Figure 4 and the slight increase in the apparent value of k_7 with increasing ClN_3 density evident in Figure 5, neither of which is reproduced by the model, suggest the onset of additional processes which contribute to the production of chain carriers. Further, the kinetic model does not agree well with NCl($a^1\Delta$) time profiles reported from a number of experiments performed at higher densities,[4,5,19] some of which exhibit secondary maxima. It may well be that under such circumstances the rates of chain propagation processes are accelerated by temperature increases, or that chain branching reactions play a greater role. We note also that the rate constants for vibrational energy exchange between $N_2(v)$ and ClN_3 might be greater for higher vibrational levels of N_2 where the energy gap is more resonant with the ClN_3 ν_2 frequency. For very small energy defects, the rate constant k_9 might approach the value for k_{-e}, i.e., 5.8×10^{-13} cm^3 s^{-1}.

Conclusions

The rate constant for quenching of $N_2(v)$ by ClN_3 is $k_9 = (2 \pm 1) \times 10^{-13}$ cm^3 s^{-1} at 300 K. This value is in keeping with a vibration-to-vibration energy transfer process, and indeed emission from vibrationally excited $ClN_3(\nu_2)$ is observed. A relatively simple model for the chain decomposition of ClN_3 carried by photofragments NCl($a^1\Delta$) and $N_2(v)$ produces computed NCl($a^1\Delta$) and ClN_3 time profiles in reasonable agreement with experiment. The model appears to underestimate the rate of the chain in the regime of higher densities of chain carriers.

Acknowledgment. This work was sponsored by the U.S. Air Force Office of Scientific Research under grant number F49620-97-0036. We are very grateful to Professor M. C. Heaven and co-workers at Emory University for sharing data prior to publication, and for numerous helpful discussions.

References and Notes

(1) Bu, Y.; Lin, M. C.; Fu, L. P.; Chtchekine, G. D.; Gilleland, D. G.; Chen, Y.; Ralph, S. E.; Stock, S. R. *Appl. Phys. Lett*. **1995**, *66*, 2433.

(2) Benard, D. J.; Linnen, C. J.; Harker, A.; Michels, H. H.; Addison, J. B.; Ondercrin, R. *J. Phys Chem. B* **1998**, *102*, 6010.

(3) Ray, A. J.; Coombe, R. D. *J. Phys. Chem*. **1995**, *99*, 7849.

(4) Ray, A. J.; Coombe, R. D. *J. Phys. Chem*. **1993**, *97*, 3476.

(5) Ray, A. J.; Coombe, R. D. *J. Phys. Chem*. **1994**, *98*, 8940.

(6) Benard, D. J. *J. Appl. Phys.* **1993**, *74*, 2900.

(7) Benard, D. J.; Chowdhury, M. A.; Winker, B. K.; Sedar, T. A.; Michels, H. H. *J. Phys. Chem*. **1990**, *94*, 7507.

(8) Henshaw, T. L.; Herrera, S. D.; Haggquist, G. W.; Schlie, L. A. *J. Phys. Chem. A*, **1997**, *101*, 4048.

(9) Piper, L. G. *J. Chem. Phys*. **1992**, *97*, 270.

(10) Coombe, R. D.; Patel, D.; Pritt, A. T., Jr.; Wodarczyk, F. J. *J. Chem. Phys*. **1981**, *75*, 2177.

(11) Rosser, W. A,; Wood, A. D.; Gerry, E. T. *J. Chem. Phys*. **1969**, *50*, 4996.

(12) Stephenson, J. C.; Moore, C. B. *J. Chem. Phys*. **1972**, *56*, 1295.

(13) Kovacs, M. A.; Rao, D. Ramachandra; Javan, A. *J. Chem. Phys*. **1968**, *48*, 3339.

(14) Coombe, R. D.; David, S. J.; Henshaw, T. L.; May, D. J. *Chem. Phys. Lett*. **1985**, *120*, 433.

(15) Cook, R. L.; Gerry, M. C. L. *J. Chem. Phys*. **1970**, *53*, 2525.

(16) Kovacs, M. A.; Javan, A. *J. Chem. Phys*. **1969**, *50*, 4111.

(17) Sharma, R. D.; Brau, C. A. *J. Chem. Phys*. **1969**, *50*, 924.

(18) Kommisarov, A. V.; Manke, G. C.; III; Davis, S. J.; Heaven, M. C. *Proc. SPIE*, in press.

(19) Coombe, R. D.; Van Benthem, M. H. *J. Chem. Phys.* **1984**, *81*, 2984.

(20) Clyne, M. A. A.; MacRobert, A. J. *J. Chem. Soc., Faraday Trans. 2* **1983**, *79*, 283.

(21) Combourieu, J.; LeBras, G.; Poulet, G.; Jourdain, J. L. *Proceedings of the 16th International Symposium on Combustion*; The Combustion Institute: Pittsburgh, PA, 1976.

(22) Henshaw, T. L.; Herrera, S. D.; Schlie, L. A. *J. Phys. Chem. A* **1998**, *102*, 6239.

(23) David, S. J.; Coombe, R. D. *J. Phys. Chem*. **1986**, *90*, 3260.